REST Journal on Emerging trends in Modelling and Manufacturing

Vol: 11(1), March 2025

REST Publisher; ISSN: 2455-4537 (Online)

Website: https://restpublisher.com/journals/jemm/

DOI: https://doi.org/10.46632/jemm/11/1/2

A Novel Multi Level Inverter with Reduced Component Count with Enhanced Reliability for Renewable Energy Solar System

***C. Brahamananda Babu, S. Waseem, A. Hemanth, K. Shahina, V. Govind, G. Avinash**

Annamacharya Institute of Technology & Sciences (Autonomous) Kadapa, Andhra Pradesh, India

*Corresponding Author Email: brahmi.210@gmail.com

Abstract: *This project presents a novel multi-level inverter topology designed to improve the reliability and reduce the component count in renewable energy solar system. The proposed inverter generates 7 and 11 voltage levels in symmetrical and asymmetrical configurations, respectively, with the ability to extend to 19 levels for reducing "Total Harmonic Distortion" (THD) in between (3-5%) as per IEEE standards. The inverter utilizes six unidirectional switches and one bidirectional switch, offering a versatile solution for generating both positive and negative voltage levels. Comparisons are made in terms of the number of switches, switch drivers, and blocking voltages to demonstrate the effectiveness of the proposed structure in minimizing component requirements. Additionally, the reliability of the proposed structure is thoroughly analyzed and compared with existing inverter topologies with increasing levels. Simulation results obtained via MATLAB validate the feasibility and performance of the proposed multilevel inverter, highlighting its potential for enhancing system reliability while reducing maintenance costs in renewable energy applications.*

1. INTRODUCTION

Renewable Energy and Power Electronics: In recent decades, the global demand for renewable energy sources, including solar, wind, and hydropower, has surged due to the increasing concerns over climate change and the depletion of fossil fuels. As a result, renewable energy systems have been integrated into national grids and private installations with increasing frequency. Among these systems, the efficient conversion of energy is a critical requirement to ensure maximum output while maintaining the stability and quality of the electricity produced. The inverter, a key component of renewable energy systems, plays an essential role in this energy conversion process. Inverters are responsible for converting the direct current (DC) generated by renewable energy sources, such as photovoltaic (solar) panels or wind turbines, into alternating current (AC), which is required for most electrical devices and systems. The design and efficiency of inverters are therefore central to the overall performance of renewable energy systems. A significant challenge for these inverters is the need to minimize energy losses during conversion while ensuring the output is free from high levels of harmonics, which can cause system inefficiencies and damage equipment. To address these challenges, advancements in power electronics, particularly in the design of inverters, have become a focal point for research and development. Power electronic converters are designed to maximize the performance and cost-effectiveness of renewable energy systems by ensuring reliable, high-quality power output with minimal losses. However, conventional inverter topologies often fall short in meeting the growing demand for higher efficiency, lower cost, and enhanced reliability, especially when it comes to large-scale installations. This brings attention to the concept of multilevel inverters, a technology that offers substantial improvements in power conversion efficiency and reduces the harmonic distortion in the output. Multilevel inverters are capable of producing multiple voltage levels instead of just two, resulting in smoother waveforms and reducing the Total Harmonic Distortion (THD), which is crucial for enhancing the power quality and extending the life of connected equipment. Despite the clear advantages, existing multilevel inverter topologies tend to be complex,

costly, and prone to reliability issues. As renewable energy systems continue to evolve, the demand for simpler, more reliable, and efficient inverter designs becomes increasingly pressing.

Multilevel Inverter Technology: Introduction to Multilevel Inverters: A multilevel inverter is an advanced type of power converter that synthesizes an output voltage waveform with multiple discrete levels, as opposed to the traditional two-level inverters. These inverters provide smoother AC waveforms, reducing the harmonic distortion present in the output. By generating a higher number of voltage levels, multilevel inverters reduce the need for complex filters and increase the overall quality of the electricity produced. The key feature of multilevel inverters is their ability to create a series of voltage levels through the use of several power semiconductor devices. By using these devices, multilevel inverters can generate voltages that are fractions of the DC supply voltage, allowing the output AC waveform to approximate a sine wave more closely than the stepped waveform produced by two-level inverters. This improves the system's overall efficiency, reduces losses in the form of heat, and minimizes harmonic distortion. Multilevel inverters can be categorized into three main types: Diode-Clamped Multilevel Inverters (DCMLI), Flying Capacitor Multilevel Inverters (FCMLI), and Cascade H-Bridge Multilevel Inverters (CHBMLI). Each of these topologies has its own distinct features and advantages but also comes with challenges related to component count, complexity, and reliability. Diode-Clamped Multilevel Inverter (DCMLI): In this topology, the number of voltage levels is determined by the number of diodes used in the circuit. The primary benefit of DCMLIs is their ability to maintain a constant voltage across each level, providing a balanced output. However, DCMLIs suffer from high complexity in control mechanisms, and the need for a large number of diodes increases the cost and reduces system reliability. Flying Capacitor Multilevel Inverter (FCMLI): FCMLIs utilize capacitors to maintain voltage balance across the inverter. While this topology provides greater flexibility and scalability in terms of voltage levels, it also requires complex balancing strategies for the capacitors, which can increase the design complexity and control difficulties. Cascade H-Bridge Multilevel Inverter (CHBMLI): One of the most popular topologies in use today, CHBMIs consist of multiple H-bridge units connected in series. Each unit can generate a set of voltage levels, and by combining multiple units, the inverter can produce a wide range of voltage levels. While CHBMIs provide excellent performance in terms of voltage quality, their major drawback is the large number of switches and components required, which increases the system's complexity, cost, and size. Despite the advantages of these multilevel topologies, they come with trade-offs. The higher the number of levels in the inverter, the greater the number of switches required, which increases the system's cost and makes it harder to maintain. Furthermore, the control strategies for these complex topologies can be difficult to implement, requiring sophisticated algorithms and real-time monitoring. As a result, a simpler and more efficient multilevel inverter design is highly sought after to address these challenges.

The Need for Novel Inverter Topologies: Challenges with Existing Multilevel Inverter Designs: Although multilevel inverters have made substantial improvements in terms of power quality and harmonic reduction, existing designs still face numerous challenges. A major issue is the complexity associated with their control and the need for large numbers of components, which increases both the cost and the risk of component failure. Additionally, with more switches in the design, the overall reliability of the inverter decreases. If any of the switches in the system fail, it can lead to cascading failures, leading to system downtime and costly repairs. In renewable energy systems, where reliability is critical due to their remote and often off-grid installations, minimizing component failure becomes especially important. Another issue with traditional multilevel inverters is the difficulty in reducing the Total Harmonic Distortion (THD) to acceptable levels. While higher voltage levels theoretically reduce THD, the complexity of the designs means that achieving optimal performance is not always straightforward. In many cases, the additional components needed to reduce THD result in an increase in the overall cost and size of the inverter, which is a major drawback in commercial and residential installations where cost-effectiveness is a priority. Furthermore, many multilevel inverter topologies rely on expensive components such as capacitors, diodes, and additional circuitry to handle the voltage balancing. These components add significant cost to the inverter, making them less attractive for applications where budget constraints are critical, such as in developing countries or small-scale installations.

Motivation for the Proposed Inverter Topology: Given the limitations of existing multilevel inverter topologies, the need for a new approach that reduces component count, increases reliability, and improves efficiency is clear. A simplified inverter design that maintains or even improves performance while minimizing the number of components would offer substantial benefits for renewable energy applications. This is the primary motivation behind the proposed novel inverter topology. The proposed inverter design uses a combination of six unidirectional switches and one bidirectional switch to generate 7 and 11 voltage levels in symmetrical and asymmetrical configurations. This innovative approach significantly reduces the number of components while still achieving the

necessary performance in terms of voltage levels and THD reduction. By using fewer switches and eliminating the need for complex capacitor balancing or diode networks, the proposed inverter is both cost-effective and more reliable, making it a perfect candidate for renewable energy systems where minimizing downtime and maintenance is critical. Additionally, the proposed inverter has the potential to be scaled up to 19 voltage levels, which provides greater flexibility in terms of application. The ability to extend the number of levels while maintaining a simple, reliable design gives the inverter an edge over more complex multilevel inverters, which require larger component counts as the number of voltage levels increases.

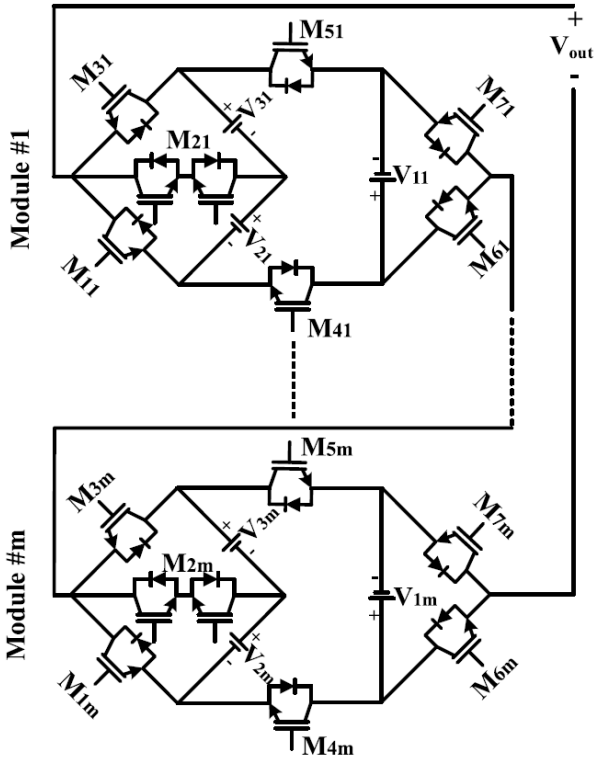

FIGURE 1. Proposed diagram of the Cascaded structure of the PMI.

2. SOLAR ENERGY

The steady increase in the level of greenhouse gas emissions and fuel costs are the main motive behind the attempt to use different sources of renewable energy [1, 2]. Among various sustainable sources of energy, the solar energy is a suitable one because it is clean, free from emission and easy to change directly to electricity utilising a photovoltaic (PV) system [2-4]. The generation of PV power has demonstrated a noteworthy potential in satisfying the demand for energy. Up to the year 2016, the worldwide operation of the sun-oriented power generation capacity has ascended to 302 GWp, which is enough to supply 1.8 per cent of the world energy demand. The solar power generation capacity has increased by nearly 100 GWp in 2017, which is about 31 per cent more from 2017 [5, 6]. However, the extensive use of a PV system is not so common because of its high starting cost. Again, there is no assurance that the energy delivered from PV exhibits steady output since it relies completely on the sun-oriented irradiance and the surrounding temperature of the PV modules, cell region, and load. For efficient operation of the PV cell under prevailing climatic conditions, an appropriate mechanism is necessary for achieving maximum power from it, which is considered as a maximum power point tracking (MPPT) in the literature. The MPPT increases the efficiency and lifetime of the PV module [7, 8]. Researchers around the world create various methodologies to take out as much power as could reasonably be expected from sustainable power sources and particularly, from the PV panels. Until now, a large number of MPPT algorithms are accessible in the literature for both off-grid and grid associated PV systems [9]. The selection of a specific MPPT system from the various existing MPPT methods is a confounding errand since every method has certain focal points and disadvantages [10]. For example, the hill climbing (HC) [11] and perturb and observe (P&O) [1, 2] methods are broadly utilised as MPPT algorithms because of their simple execution and fewer sensor necessities. The incremental conductance (INC) algorithm [12], which looks at incremental and momentary conductance of PV systems, can track the maximum power point (MPP) of a PV system and exchange high PV power to the load. The research work presented in [13] clarifies the misconception

between the widely used P&O and INC algorithms and shows that they are almost highly identical under steady-state and transient conditions. It is shown that they both have similar mathematical expression except that the INC ignores the higher-order term in the discrete differentiation of the power. The sliding control (SC) method, however, complex in equipment usage yet, is more precise than ordinary methods [14]. The classical algorithms, such as P&O, INC, HC, fuzzy logic and neural network, cannot find the global MPP (GMPP) under partial shading condition (PSC) [15]. A comparison among various global MPPT (GMPPT) methods based on meta-heuristic algorithms is given in [16]. It is concluded that particle swarm optimisation (PSO) and Cuckoo search (CuS) algorithms-based trackers ensure the convergence to the GMPP and the tracking performance of the CuS algorithm is better than the PSO. For effectively tracking the MPPT of a PV system, a model-free spline-guided Jaya algorithm is proposed in [17], which is able to perform efficiently under PSC and also provides faster convergence speed. An MPPT technique based on temperature described in [18] needs a fewer number of sensors than customary strategies. This technique is straightforward in execution and is economical too. The bisection search theorem-based MPPT, detailed in [19], is generally utilised when the PV array shows at least two neighbourhood MPPs under changing climatic conditions, where the utilisation of different methods is a troublesome undertaking. Until now, the operation of various MPPT methods is presented by various research papers. A lot of research works have also been published to classify these methods. Research works in [2] present a categorisation approach for MPPT methods based on three categories such as off-line, online and hybrid methods. The research work in [20] categorises the MPPT methods as analogue, digital, and hybrid methods and provides a comparison based on only five selection parameters. In [21], the MPPT methods are categorised into five categories based on their tracking techniques and the comparison that is given based on five selection parameters. These available categorisation methods cannot classify all the available methods appropriately and the available comparison among the MPPT methods does not consider all the available selection parameters. An endeavour is made in this study to categorise the discussed 50 MPPT methods into eight categories based on their tracking nature and manipulation techniques for finding the true MPP. The categorised eight groups are conventional methods, methods based on mathematical calculations, constant parameters-based methods, measurement and comparison-based methods, trial and error-based methods, numerical methods, intelligent prediction-based methods, and methods based on iterative in nature. To find out the efficient method among others, a tabular comparison is also done in each category based on 11 selection parameters. The considered 11 selection parameters are design complexity, sense parameters, PV array dependency, prior training, periodic tuning, convergence speed, analogue/digital in nature, cost, tracking true MPP, stability, and efficiency of the system. These comparison tables and ways of categorisation will be helpful in future for selecting appropriate MPPT methods for the solar PV system.

Model of PV cell

The model of a solar PV cell is an important part of analysing a PV system. Its modelling is classified into three sections, which are described below.

I-V characteristics and equivalent circuit

PV begins from two separate words – photo, which implies light, and voltaic, which alludes to the production of power [22]. Subsequently, the term PV brings the significance of producing power specifically from the sun. A sun-powered array comprised several combinations of sun-based modules, where every module comprised various solar cells [1]. Solar cells comprise p–n diodes manufactured in a thin layer of semiconductor [23]. They resemble p–n diodes and their attributes are additionally comparative. Fig. 1 displays the equivalent circuit of a perfect PV cell [1]. This ideal structure is sufficiently precise to comprehend the PV attributes and the reliance of the PV cell on varying climatic conditions [20].

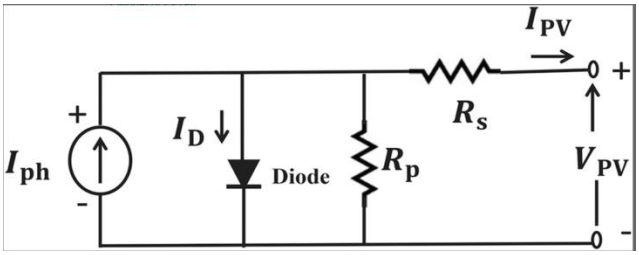

FIGURE 2. Equivalent circuit of a solar panel [**1**]

The aggregate output current of the parallel and series connected PV modules is expressed in (1) [24]

$$I_{PV} = N_p\left(I_{ph} - I_o\left[\exp\left(\frac{q(V_{PV}+R_sI_{PV})}{N_sAKT}\right)-1\right]-\frac{V_{PV}+R_sI_{PV}}{N_sR_p}\right),$$

where Ipv is the output current, Vpv is the output voltage, Rs is the series resistance, Rp is the parallel resistance, Np and Ns are the number of PV cells connected in parallel and series for a given PV module, A is the ideality factor of the p–n junction, K is the Boltzmann's constant (1.3806503 x 10^{-23}J/K), T is the temperature in Kelvin, q is the charge of electron (1.6x10^{-19}C) [24], Iph is the produced photocurrent; it depends fundamentally on the radiation and cell's temperature, which is expressed as

$$I_{ph} = [I_{SCC-STC} + K_i(T - T_{STC})]\frac{G}{G_{STC}},$$

where Iscc-stc refers to the short-circuit current (SCC) at standard test conditions (STC) in amperes, Tst (25^0C) is the cell temperature at STC, G (in watts per square meters,) is the irradiation on the cell surface, Gstc(1000W/m^2) is the irradiation at STC and is the SCC coefficient, as a rule, given by the cell producer. In addition, the saturation current, , is impacted by the temperature as indicated by the accompanying equation [25, 26]

$$I_o = \frac{I_{SCC-STC} + K_i(T - T_{STC})}{\exp[(V_{OCV-STC} + K_v(T - T_{SCC})/AV_{th})]},$$

where (Vocv-stc in volt, V) is the open circuit voltage (OCV) at STC, Kv is the OCV coefficient, Vth refers to the thermal voltage of the cell, these values are available on the data sheet provided by module's manufacturer. With Vpv and simplified Ipv, the power produced by the PV module is represented as [24]

$$P_{PV} = V_{PV} \times N_p\left(I_{ph} - I_o\exp\left(\frac{qV_{PV}}{N_sAKT}\right)-\frac{V_{PV}}{N_s}\right).$$

The I-V and P-V characteristics curve of the solar cell is shown in Fig. 2 [2]. The curve in this figure indicates that the operating point of the PV does not remain at a stable point; it actually varies from zero to open-circuit voltage. There is only one point, which enables maximum power for a given set of solar insolation and temperature level. That particular point is indicated as MPP and at that point, the current and voltage that are found are presented as Impp and Vmpp in Fig. 2. This significant MPP and its numerous tracking methods are the main focal point of this review work.

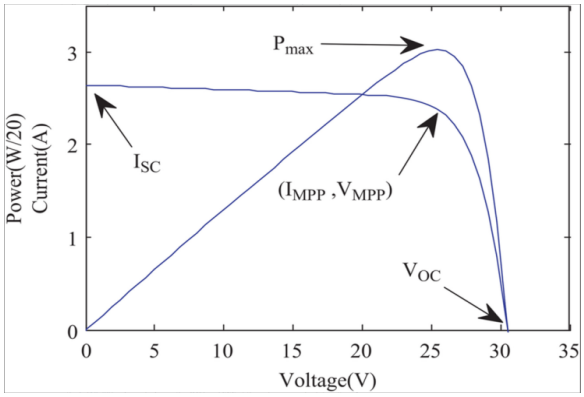

FIGURE 3. I-V and P-V curve of a PV cell [2]

3. EFFECT OF IRRADIANCE AND TEMPERATURE

The output of PV shifts with the changing climatic conditions [27, 28]. Since the irradiance of the solar cell relies upon the incidence angle of the sunbeams, this parameter straightforwardly influences the output adjusting the P-V and I_V characteristics [20]. The output current, Ipv, of a PV module is broadly impacted by a variety of sun-oriented irradiance, G, though the output voltage, Vpv, remains practically constant. On the other hand, for a changing temperature, it is found that the voltage shifts generally while the current remains practically unaltered [9]. The temperature of the PV cell increases because of three reasons: (i) its own heat amid PV activity, (ii) the energy emanated at the infrared wavelength, which has a warming impact on the cell, and (iii) an increase in sunlight-based

insolation [10]. The OCV, Voc, and SCC, Isc, are found by (5) and (6), respectively, of PV array at sun intensity and cell temperature, where the sun intensity (insolation) is measured in W/m^2

$$V_{OC} = V_{OC}^{*} + a_2(T - T^{*}) - (I_{SC} - I_{SC}^{*})R_s,$$

$$I_{SC} = I_{SC}^{*}\left(\frac{G}{G^{*}}\right) + a_1(T - T^{*}).$$

In (5) and (6), a1 and a2 are the PV cell temperature coefficients for current and voltage, respectively [10, 29]. V*oc and I*sc are the OCV and SCC at the reference solar intensity G* and T* temperature. The photo-current, Iph, and henceforth the PV panel SCC relies upon the insolation and temperature, which suggests that as radiations increment, the current and subsequently, power, i.e. maximum power increments and vice-versa [30, 31]. For solving this, the MPPT is introduced for locating the MPP with the variation in temperature and irradiance.

4. PROPOSED MULTILEVEL INVERTER (PMI) STRUCTURE

The structure of the PMI is shown in Fig. 1. This inverter needs seven power switches (six unidirectional switches and one bidirectional switch) and three dc sources. Switching states of the PMI structure are depicted in Fig. 2(a)–(f). The dc sources can be provided through photovoltaic cells, batteries, or fuel cells. Therefore, the PMI is a good candidate for renewable energy resources. In applications where one dc source is available, the PMI structure may not be a good candidate such as ac drive motors when supplied by rectifiers. The PMI structure can be implemented by symmetrical and asymmetrical configurations. Therefore, it has three different operating cases as follows:

- Case A: if V1 = V2 = V3 = E, the PMI structure generates a seven-level output voltage waveform.
- Case B: if V1 = 3E and V2 = V3 = E, the PMI structure generates an 11-level output voltage waveform.
- Case C: if V1 = V3 = E and V2 = 2E, the PMI structure generates a nine-level output voltage waveform.

In the PMI structure, only three conducting switches are to generate each voltage level. However, in seven-level structures of CHBI, FCI, and NPCI six conducting switches are needed. One main concept in the PMI structure is using all the capabilities of the utilized dc sources to generate positive and negative levels and remove the need for H-bridge structure. The structure is designed in a smart way to prevent connecting the positive pole of any dc source to the anode of any diode. Therefore, this will result in preventing any unexpected current flowing through the structure. Also, the switching states presented in Table I are selected in a way that prevents dc sources make any closed loop. As can be seen in Table I, two switches M4 and M5 operate in the line frequency. This also causes further reduction in the switching losses and increase in the efficiency. The maximum standing voltage (MSV) of the switches M1–M7 in the PMI structure are V2 + V3, V2 + V3, V2 + V3, V1 + V2+ V3, V1 + V2 + V3, V1, and V1, respectively. It should be noted the bidirectional switch M2 is considered as two one directional switches that one switch should block the voltage of V2 in one direction and the other one should block the voltage of V3 in the reverse direction. The TSV of the switches in the PMI structure is equal to the sum of all the MSV of the switches M1–M7 and can be obtained through the following equation:

$$\begin{aligned} \text{TSV} &= 3(V_2 + V_3) + 2(V_1 + V_2 + V_3) + 2(V_1) \\ &= 4V_1 + 5V_2 + 5V_3 \end{aligned}$$

TABLE 1. Switching States Of The Pmi Structure

V_{out}	M_1	M_2	M_3	M_4	M_5	M_6	M_7
0	0	0	1	0	1	0	1
	1	0	0	1	0	1	0
V_1	1	0	0	1	0	0	1
V_2	0	1	0	1	0	1	0
V_1+V_2	0	1	0	1	0	0	1
V_2+V_3	0	0	1	1	0	1	0
$V_1+V_2+V_3$	0	0	1	1	0	0	1
$-V_1$	0	0	1	0	1	1	0
$-V_3$	0	1	0	0	1	0	1
$-V_1-V_3$	0	1	0	0	1	1	0
$-V_2-V_3$	1	0	0	0	1	0	1
$-V_1-V_2-V_3$	1	0	0	0	1	1	0

5. EXTENDED STRUCTURE OF THE PMI

The PMI structure can be extended through different ways to produce higher number of voltage levels. This is an outstanding feature of the PMI. It can get extended from the right side or left side of the PMI. Another possible solution is obtained by cascading the PMI structure. For the sake of simplicity, only this solution is studied here. Fig. 3 shows the cascaded structure of the PMI (CSPMI). This structure is a good choice for applications such as photovoltaic farms, where cumulative dc sources are available. The number of switches, NSW, the number of dc sources, NDC, and the relation between NSW and NDC for m modules can be calculated through (2)–(4), respectively. It should be noted that the bidirectional switches are considered as two switches

$$N_{\mathrm{SW}} = 8m$$
$$N_{\mathrm{DC}} = 3m$$
$$N_{\mathrm{SW}} = 8N_{\mathrm{DC}}/3$$

Another good point of the CSPMI is that the MSV of the switches is not changed when the number of levels is increased. Therefore, the TSV for the CSPMI, for m modules, can be calculated through the following equation:

$$\begin{aligned}\mathrm{TSV} &= 2m(V_2+V_3)+2m(V_1+V_2+V_3)+2m(V_1)+mV_3\\ &= 4mV_1+4mV_2+5mV_3\end{aligned}$$

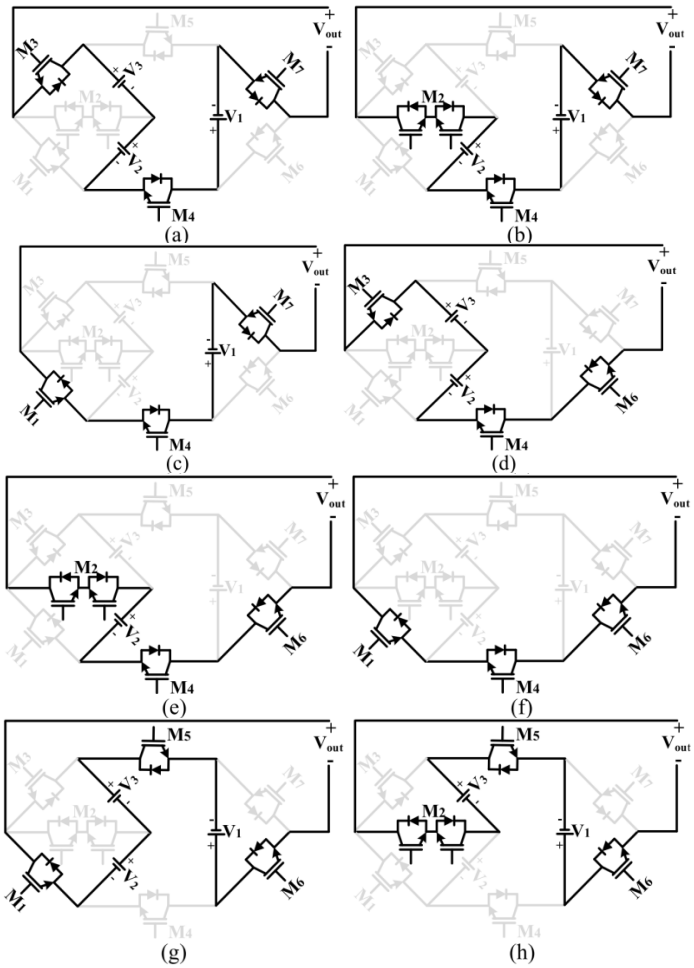

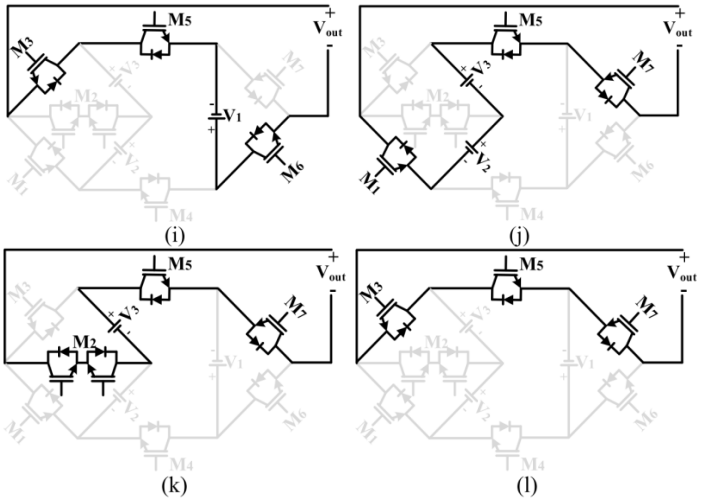

FIGURE 4. Different switching states of the PMI structure. (a) State V1+V2+V3. (b) State V1 + V2. (c) State V1. (d) State V2 + V3. (e) State V2. (f) State 0. (g) State −V1−V2−V3. (h) State −V1−V3. (i) State −V1. (j) State −V2−V3. (k) State −V3. (L) State 0.

The CSPMI can be implemented in both symmetrical and asymmetrical configurations. These two cases are studied in the following.

Case 1: Symmetrical CSPMI In the symmetrical CSPMI, the maximum number of levels, NL, and the relation between NSW and NL for the CSPMI can be found through (7), and (8), respectively

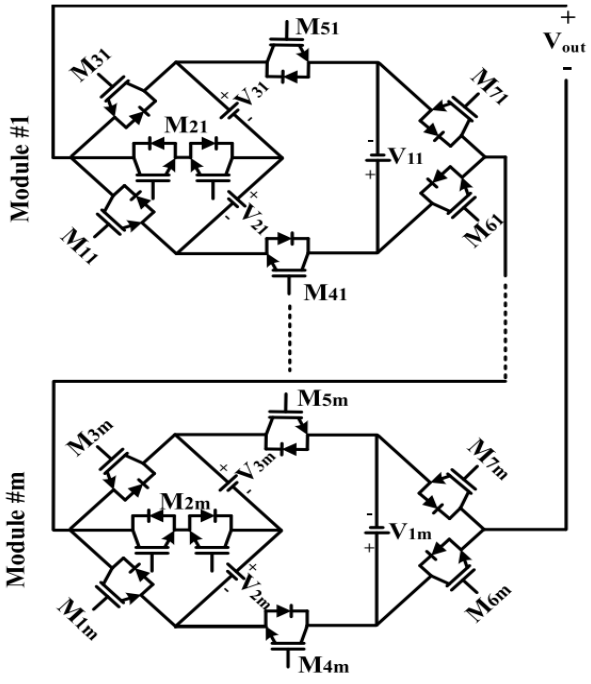

FIGURE 5. Cascaded structure of the PMI.

$$V_{11} = V_{21} = V_{31} = E$$
$$V_{12} = V_{22} = V_{32} = E$$
$$\vdots$$
$$V_{1m} = V_{2m} = V_{3m} = E$$
$$N_{\mathrm{L}} = 2 \times (3m) + 1 = 6m + 1$$
$$N_{\mathrm{SW}} = (8N_{\mathrm{L}} - 8)/6$$

These equations and following equations are used in the comparison section.

Case 2: Asymmetrical CSPMI In the asymmetrical CSPMI, the proposed inverter can operate under two different modes. In the mode I, the dc sources V1m,..., V11 have an equal voltage amplitude of 3E, and dc sources V2m, V3m,..., V21, V31 have an equal voltage amplitude of E. In the mode II, the amplitude of dc sources V1m,..., V11 are equal to the maximum number of produced levels in the previous module times E and the amplitude of dc sources V2m, V3m,..., V21, V31 are equal to three times of V1m,..., V11 amplitude. The related equations of mode I and mode II are presented in (9)–(11) and (12)–(14), respectively

Mode I

$$V_{21} = V_{31} = E \;\; \& \;\; V_{11} = 3V_{22} = 3V_{32} = 3E$$
$$V_{22} = V_{32} = E \;\; \& \;\; V_{12} = 3V_{22} = 3V_{32} = 3E$$
$$\vdots$$
$$V_{2m} = V_{3m} = E \;\; \& \;\; V_{1m} = 3V_{2m} = 3V_{3m} = 3E$$
$$N_{\mathrm{L}} = 10m + 1$$
$$N_{\mathrm{SW}} = (8N_{\mathrm{L}} - 8)/10$$

Mode II

$$V_{21} = V_{31} = E \;\; \& \;\; V_{11} = 3V_{22} = 3V_{32} = 3E$$
$$V_{22} = V_{32} = (V_{11} + V_{21} + V_{31}) = 5E \;\; \& \;\; V_{12} = 3V_{22} = 3V_{32} = 15E$$
$$\vdots$$
$$V_{2m} = V_{3m} = (V_{1(m-1)} + V_{2(m-1)} + V_{3(m-1)}) = 5^{(m-1)}$$
$$V_{1m} = 3V_{2m} = 3V_{3m} = 3 \times 5^{(m-1)}$$
$$N_{\mathrm{L}} = 11^{m}$$
$$N_{\mathrm{SW}} = 8 \log_{11}^{N_{\mathrm{L}}}$$

6. SIMULATION RESULTS

The simulations carried out using the MATLAB/Simulink software to investigate the performance of the PMI structure. The utilized modulation technique is the level shifted sinusoidal pulse width modulation.

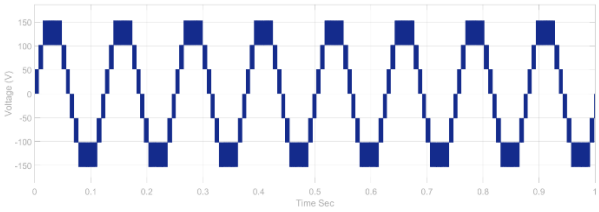

(a)

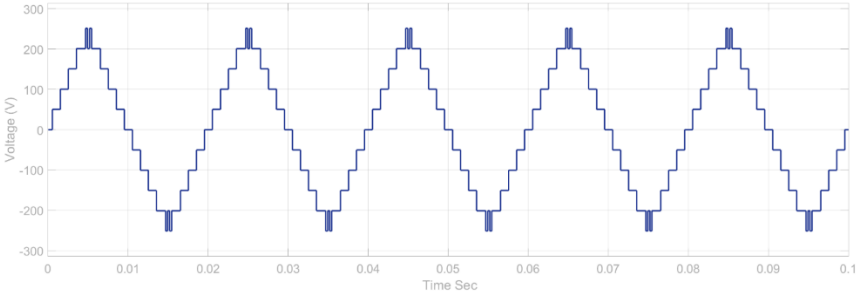

(b)

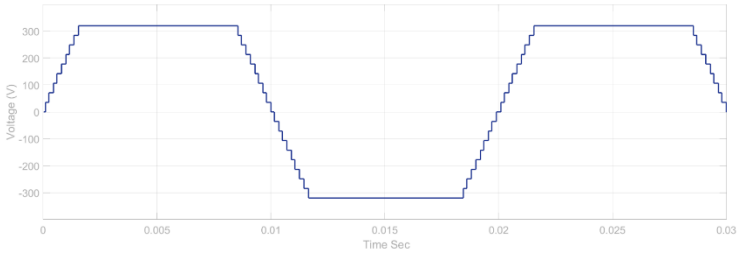

(c)

FIGURE 6. 9(a), (b) and (c) shows the output voltage and current of the PMI structure when it operates as a 7-level inverter and as an 11-level inverter, and 19 level respectively. It should be mentioned that the harmonics analysis is a direct performance index associated with multilevel topologies.

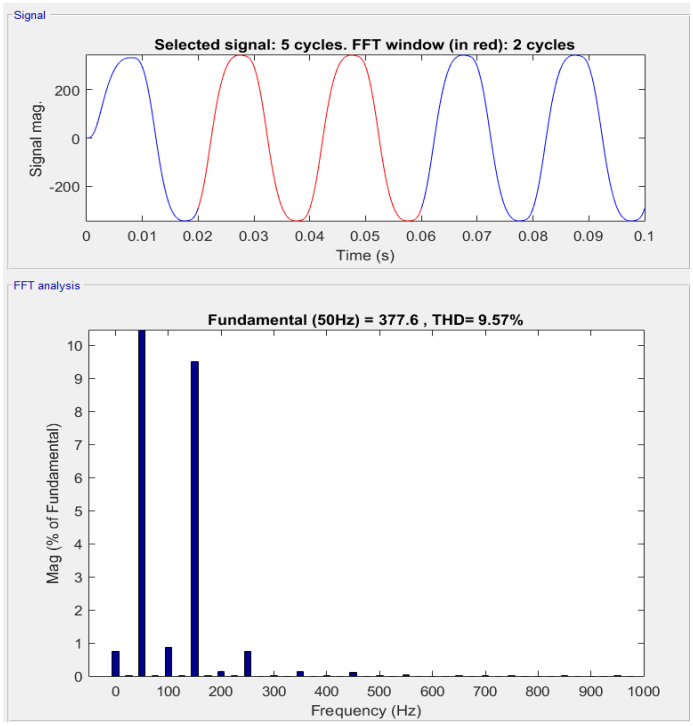

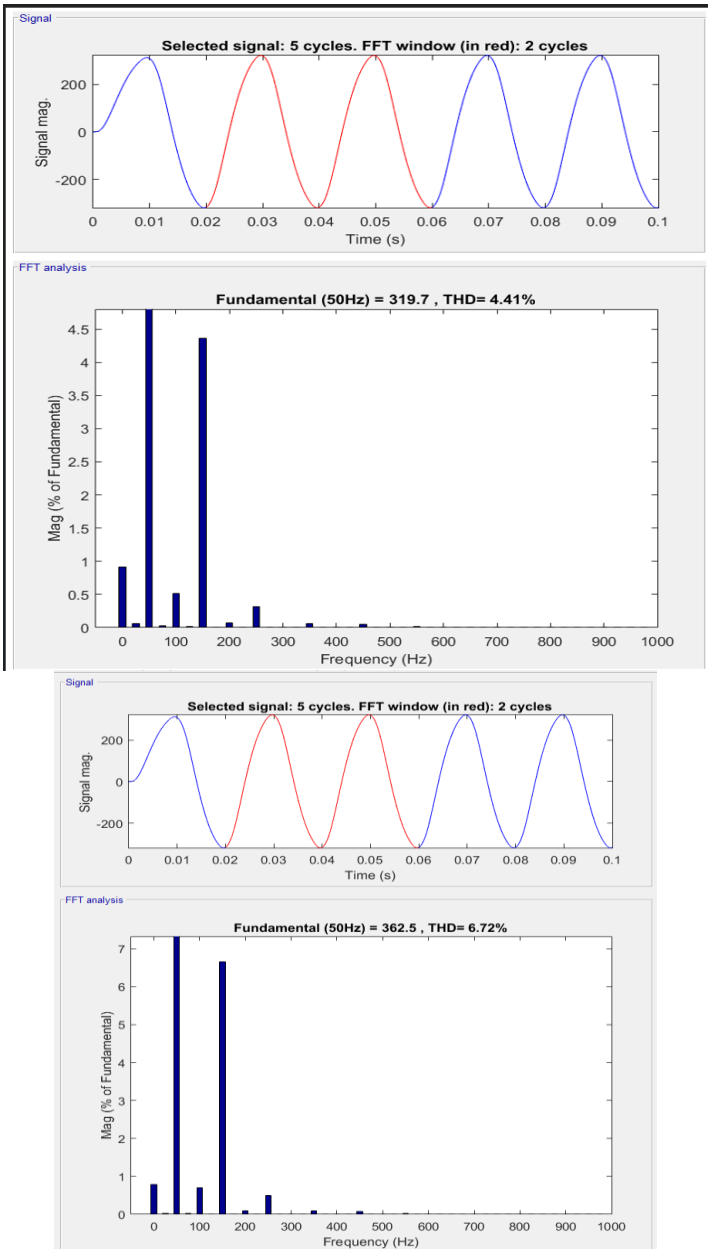

FIGURE 7. shows the fast Fourier transform (FFT) of the 7 level 11-level and 19 level output voltage waveforms. The output voltage THD for the output voltage is 9.57, 6.27 and 4.41% respectively.

So, by employing a simple LC filter, the main component can be extracted easily. This is a good point of this modulation technique. Also, it should be noted that the same modulation scheme and the same number of voltage levels in different inverters structures result in similar harmonic components and THD. Therefore, the harmonic components are not studied in comparison of different structure with the same number of voltage levels.

7. CONCLUSION AND FUTURE SCOPE

This article introduces a groundbreaking improvement in the structure of multilevel converters for applications involving multiple DC sources, such as renewable energy systems, including solar photovoltaic (PV) power. The proposed inverter structure delivers up to 19 voltage levels with a reduced number of components, contributing to a more compact and cost-effective solution for integrating renewable energy. Additionally, the multiport inverter (PMI) design operates efficiently under both symmetrical and asymmetrical conditions, offering flexibility across a

broad range of applications. This scalability allows the PMI structure to generate any desired number of voltage levels, making it an ideal option for high-voltage applications and renewable energy sources like solar PV systems.
The article also emphasizes the evaluation of the PMI structure's reliability, which is a critical factor for practical implementation. Key parameters for assessing the reliability of multilevel inverter designs are discussed, including the number of switches, gate drivers, total blocking voltage, and efficiency. Comparisons between the PMI structure and conventional multilevel inverters reveal that the proposed inverter offers superior reliability with fewer switches, thereby simplifying the system and improving long-term performance. Simulation results demonstrate the PMI structure's effectiveness in renewable energy systems and high-voltage applications, showing its potential for enhancing energy conversion efficiency, system reliability, and cost-effectiveness. Notably, the inverter produces a total harmonic distortion (THD) of only 4.41%, further showcasing its efficiency and performance. The integration of this inverter into renewable energy systems, particularly in solar PV applications, marks a significant advancement in creating scalable and efficient energy solutions. Future work should focus on optimizing control strategies and developing advanced features to further enhance the PMI structure's performance in real-world renewable energy applications.

REFERENCES

[1]. A. Salem, H. Van Khang, K. G. Robbersmyr, M. Norambuena, and J. Rodriguez, "Voltage source multilevel inverters with reduced device count: Topological review and novel comparative factors," IEEE Trans. Power Electron., vol. 36, no. 3, pp. 2720–2747, Mar. 2021.

[2]. Q. Liu, T. Caldognetto, and S. Buso, "Review and comparison of gridtied inverter controllers in microgrids," IEEE Trans. Power Electron., vol. 35, no. 7, pp. 7624–7639, Jul. 2020.

[3]. A. Akbari, F. Poloei, and A. Bakhshai, "A brief review on state-of-theart grid-connected inverters for photovoltaic applications," in Proc. IEEE 28th Int. Symp. Ind. Electron. (ISIE), Vancouver, BC, Canada, Jun. 2019, pp. 1023–1028.

[4]. J. Ebrahimi and H. Karshenas, "A new single DC source six-level flying capacitor based converter with wide operating range," IEEE Trans. Power Electron., vol. 34, no. 3, pp. 2149–2158, Mar. 2019.

[5]. S. Kouro et al., "Recent advances and industrial applications of multilevel converters," IEEE Trans. Ind. Electron., vol. 57, no. 8, pp. 2553–2580, Aug. 2010.

[6]. M. Vijeh, M. Rezanejad, E. Samadaei, and K. Bertilsson, "A general review of multilevel inverters based on main submodules: Structural point of view," IEEE Trans. Power Electron., vol. 34, no. 10, pp. 9479–9502, Oct. 2019.

[7]. J. Ebrahimi and H. Karshenas, "A new modulation scheme for a fourlevel single flying capacitor converter," IEEE Trans. Ind. Electron., vol. 68, no. 3, pp. 1860–1870, Mar. 2021.

[8]. W. Li, Y. Gu, H. Luo, W. Cui, X. He, and C. Xia, "Topology review and derivation methodology of single-phase transformerless photovoltaic inverters for leakage current suppression," IEEE Trans. Ind. Electron., vol. 62, no. 7, pp. 4537–4551, Jul. 2015.

[9]. E. Samadaei, A. Sheikholeslami, S. A. Gholamian, and J. Adabi, "A square T-type (ST-type) module for asymmetrical multilevel inverters," IEEE Trans. Power Electron., vol. 33, no. 2, pp. 987–996, Feb. 2018.

[10]. E. Samadaei, M. Kaviani, and K. Bertilsson, "A 13-levels module (Ktype) with two DC sources for multilevel inverters," IEEE Trans. Ind. Electron., vol. 66, no. 7, pp. 5186–5196, Jul. 2019.